Weierstraß-Institut für Angewandte Analysis und Stochastik

Leibniz Gemeinschaft

Numerical Simulation of Czochralski Crystal Growth

April 28, 2008

Ch. Lechner, O. Klein, P.-E.-Druet, W. Dreyer, J. Sprekels

in collaboration with the Institute of Crystal Growth (IKZ)
Ch. Frank-Rotsch, F. Kießling, D. Jockel, P. Lange, W. Miller, U. Rehse, P. Rudolph, M. Ziem

Plan

- Introduction
- Numerical Methods
- Comparison to experiments
- Current investigations
- Summary

Plan

- Introduction
  - Growth of GaAs by the Czochralski method
  - Traveling magnetic fields
  - Current investigations
- Numerical Methods
- Comparison to experiments
- Current investigations
- Summary

Introduction: Growth of GaAs by the Czochralski Method

Czochralski method:

- technique to grow large mono-crystals from the melt
  - semi-conductors (Si, Ge, GaAs), metals, oxides, halides

  GaAs
- semi-conductor mono-crystals
  - Si: $\varnothing \sim 200 - 300$ mm, length $\sim$ m
  - GaAs: $\varnothing \sim 100 - 150$ mm
  - crystal (cylinder) is cut into wafers $\rightarrow$ substrate for chips

improve process: increase growth yield, improve quality of crystal
additional instrument to control the process: magnetic fields

KRISTMAG

develop a new technology for applying traveling magnetic fields

Growth of GaAs by the Czochralski method

Liquid Encapsulated Cz (LEC)

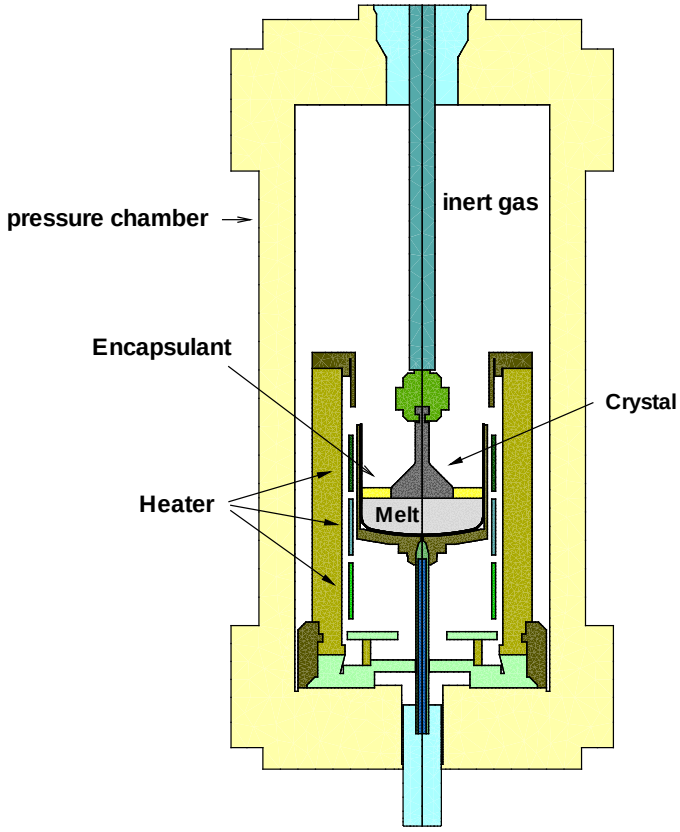

Vapor pressure controlled Cz (VCz)

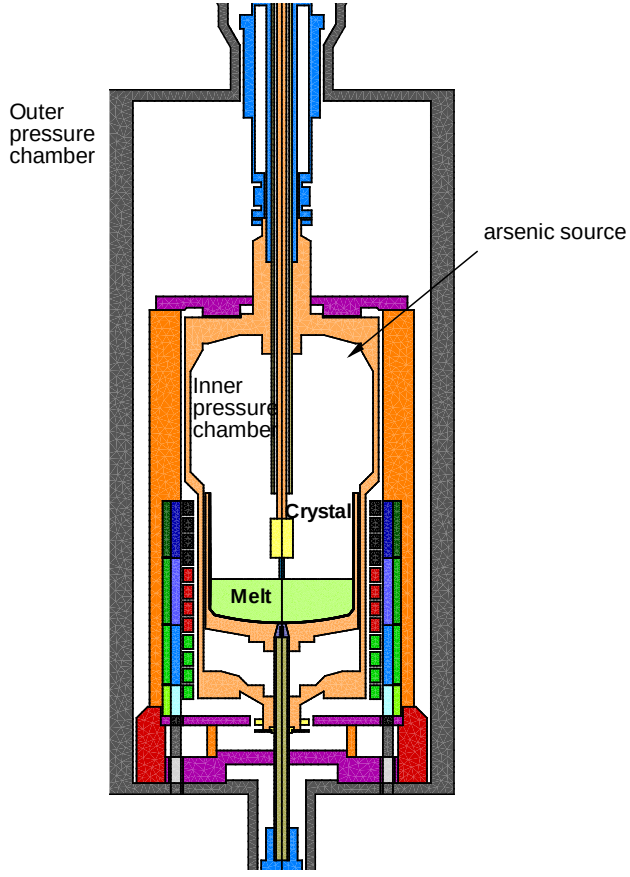

Crystal and melt – melt flow and temperature fluctuations

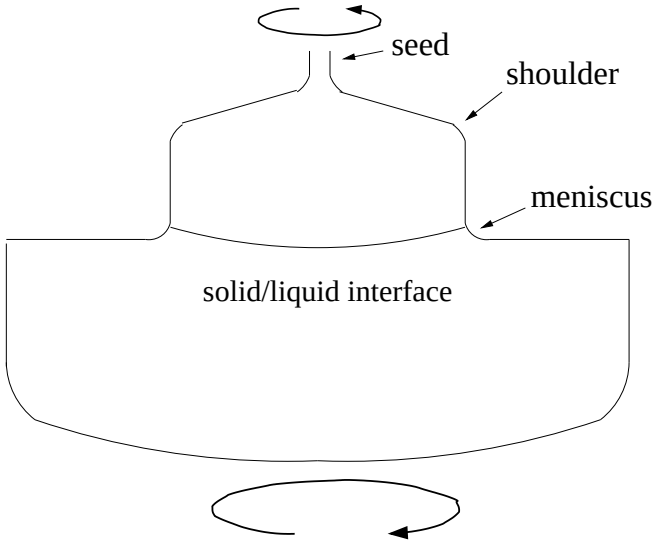

- solid/liquid interface: konvex, nearly planar
- meniscus influences diameter, thermally controlled
- release of latent heat, limits pull velocity

convection due to buoyancy has to be controlled

- rotation of crystal : homogenize radial temperature distribution
- rotation of crucible: stabilize flow, damp convection

increase growth yield ($\Rightarrow$ melt height)

- need additional instrument to control the melt flow and temperature fluctuations, e.g. magnetic fields

Traveling magnetic field

alternating current: frequency f, phase shift between coils ϕ

infinite conductor

$$\vec{A} = A(r)e^{i(2\pi f t - az)}\vec{e}_\varphi$$

a wave number, $a \propto \phi$

$f \geq 50\,\text{Hz} \Rightarrow$ average $\vec{F}_L$ over a period

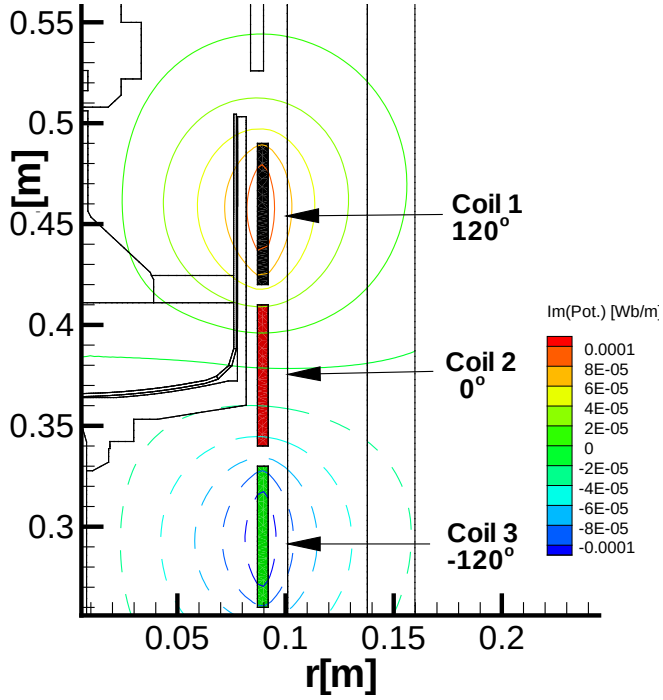

$f = 50\,\text{Hz}, 120^0$ down

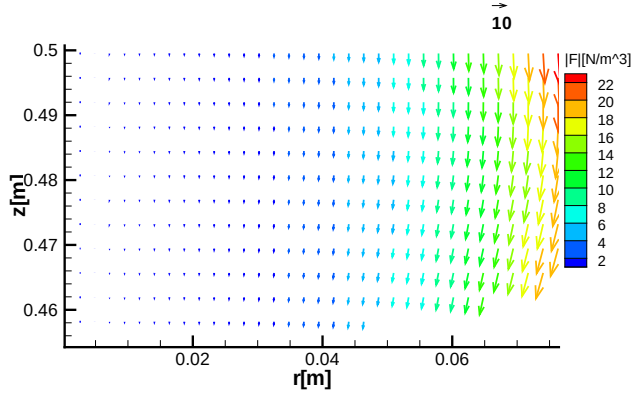

vertical component of $\vec{F}_L$ counteracts buoyancy

Parameters

$\vec{F}_L$ strongly depends on frequency f and phase shift ϕ, e.g.

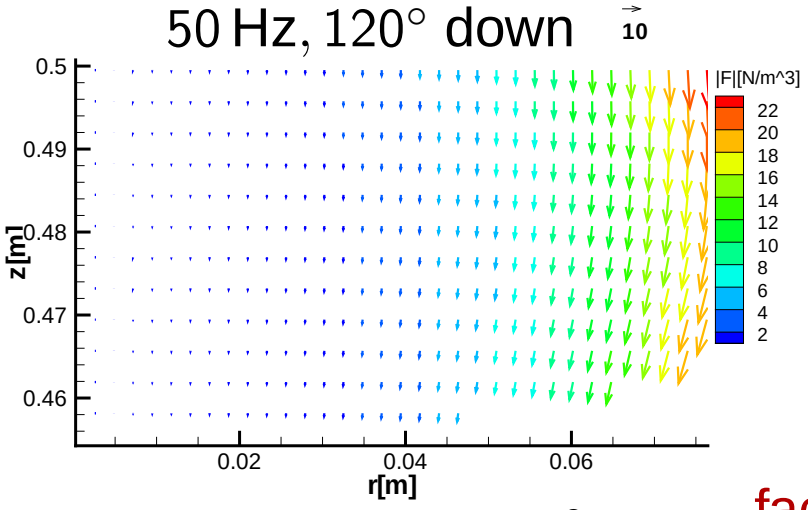

$|F|_{\max} = 23.8\,\mathrm{N/m^3}$

factor 13

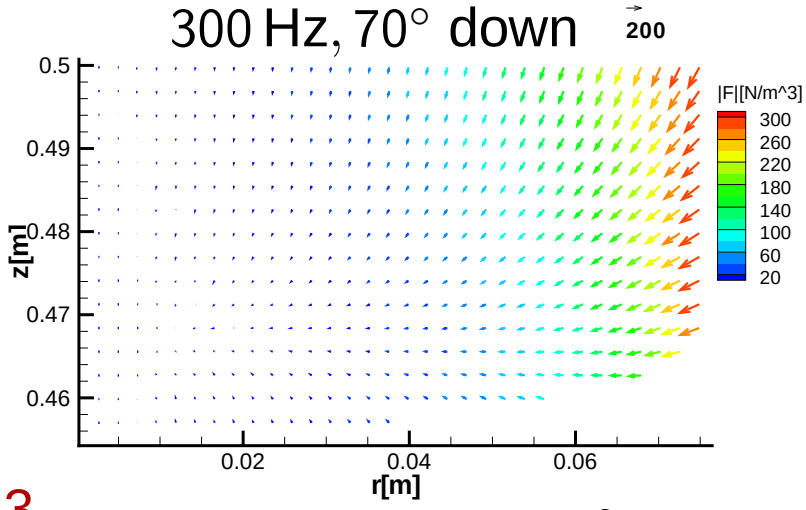

$|F|_{\max} = 317.7\,\mathrm{N/m^3}$

$\Rightarrow$ additional parameters in the growth process

New technology

usually
induction coils outside

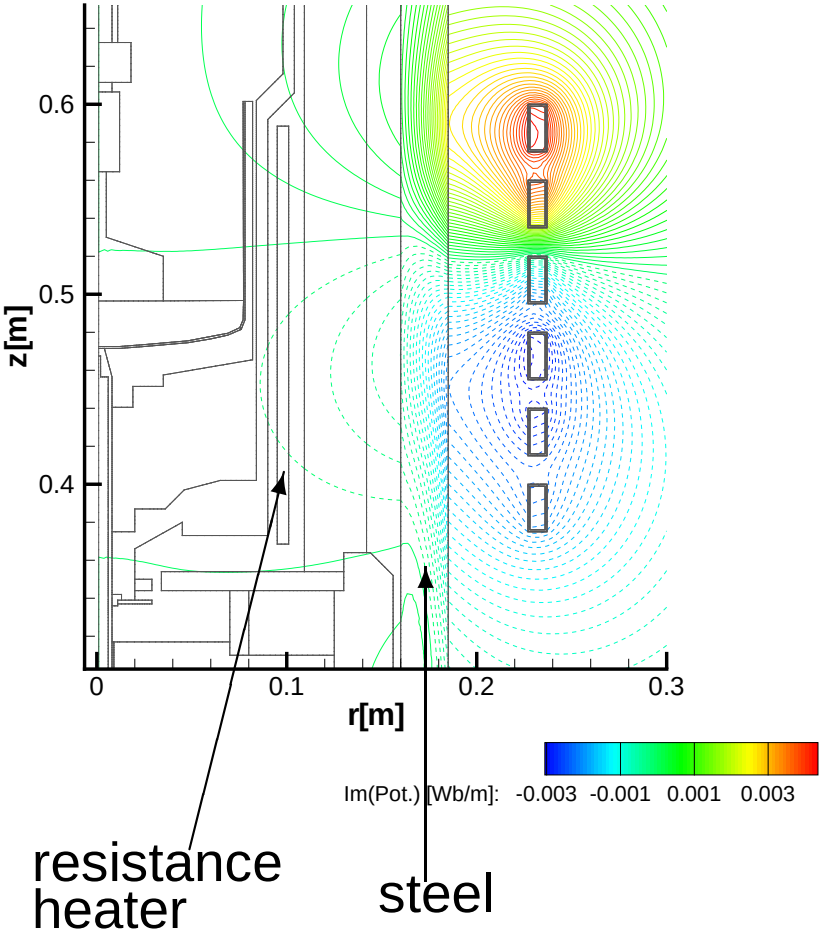

combined heater magnet module

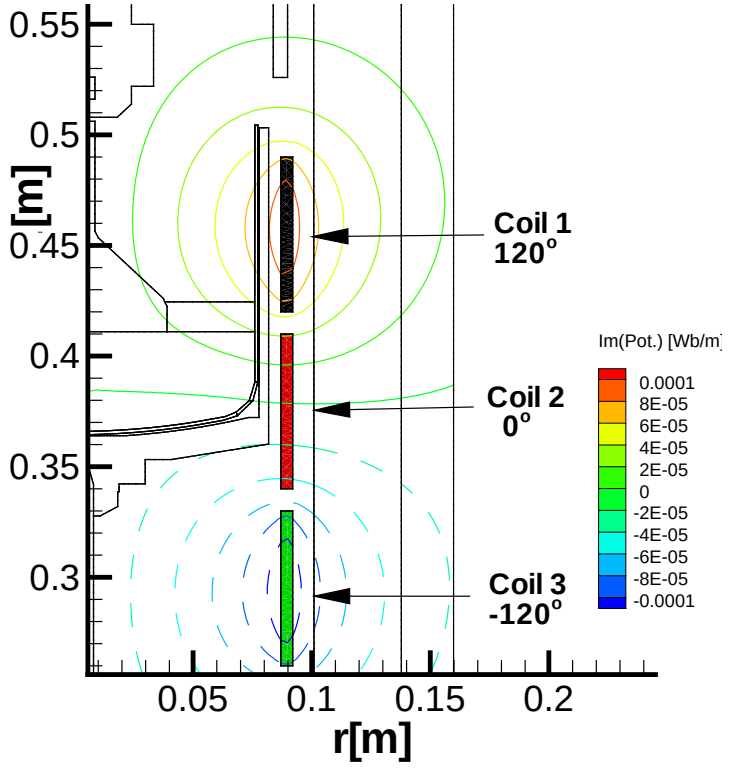

reduces power consumption

$\sim$ 9 kW produce a relevant field

Development of the new technology

experiment

- crystal growth is possible with the new module
  - VCz without boron oxide: several crystals grown
  - LEC: first crystals
- influence of the magnetic field
  - VCz: influence shown
- magnetic field improves growth process
  - VCz: striations more regular with smaller amplitude

tasks for numerics

- simulations to “aid the design”, limit parameter ranges, e.g.
  - thickness of coils $\Rightarrow$ Lorentz force
  - reduce temperature oscillations close to the interface
- reproduce experimental results, provide explanations, e.g.
  - Lorentz force: experiment $\leftrightarrow$ simulation
  - comparison with results from VCz growth

Plan

- Introduction
- Numerical Methods
  - Overview
  - Maxwell equations
  - Global, stationary temperature distribution
  - Local simulation: Navier-Stokes
- Comparison to experiments
- Current investigations
- Summary

Numerical Methods – Overview

Global simulation
stationary

- magnetic field, currents: reduced Maxwell equations
- temperature distribution
  - heat conduction
  - radiation
  - heat sources
- control T at triple point
- axially symmetric
- WIAS-HiTNIHS (Klein, Philip)
  - finite volume method
  - pdelib, PARDISO, triangle

Coupling

$\longrightarrow$

$T_{stat}, \vec{F}_L$

Local simulation
transient

- Navier-Stokes equations Boussinesq approx. $\Rightarrow u, p, T$ in the melt
- $\vec{F}_L$, boundary data for T from global simulation
- axially symmetric, 3D
- Large Eddy Simulations
- NAVIER (Bänsch)
  - finite element method
  - fractional θ scheme

What we neglect ...

- solid/liquid interface
  - a-priory given flat interface between crystal and melt
    $\Rightarrow$ no statements about the interface possible
- gas convection
  - input power is underestimated
  - error depends on the growth method
    VCz with B_2O_3: good reproduction of axial temperature gradients
    VCz without B_2O_3 ?
    LEC: e.g. heating power strongly depends on pressure
- global simulation: convection of the melt
  - overestimates input power and ΔT in the melt
  - high rotation rates: rotation dominates convection

What we neglect ...

- motion induced current
  - $\vec{j} = \sigma(\vec{E} + \vec{u} \times \vec{B})$
  - dimensional analysis: $\frac{|\vec{u} \times \vec{B}|}{|\vec{E}|} \sim 10^{-3}$
  - Maxwell equations decouple from Navier-Stokes
- global simulation: assumption of axial symmetry
  - heater magnet module deviates from axial symmetry $\rightarrow$ approximate 3D effects in 2D simulation
  - asymmetry of magnetic field is compensated by rotation of the melt
- local simulation: assumption of axial symmetry
  - in the vicinity of the axis: severe
  - in the outer part of the crucible: rotation stabilizes flow

Global Simulation – Magnetic field

Maxwell's equations (neglecting the displacement current $\partial_t \vec{D}$):

$$\vec{\nabla} \times \vec{H} = \vec{j} \tag{1}$$

$$\vec{\nabla} \vec{B} = 0 \qquad \partial_t \vec{B} + \vec{\nabla} \times \vec{E} = 0 \tag{2}$$

Ohm's law $\vec{j} = \sigma \vec{E}$

assumptions:

- axially symmetric setting,

$$\vec{j} = j \vec{e}_\varphi, \quad \vec{A} = \phi \, \vec{e}_\varphi, \quad \text{where} \quad \vec{B} = \vec{\nabla} \times \vec{A}$$

- all electro-magnetic quantities are periodic in time

reduced Maxwell equations:

$$-\frac{1}{\mu} \vec{\nabla} \cdot \left(\frac{\vec{\nabla}(r\phi)}{r^2} \right) = \frac{j}{r}, \qquad j = \begin{cases} 0 & \text{in insulators,} \\ -i\omega \, \sigma_c \, \phi + \frac{\sigma_c \, v_k}{2\pi r} & \text{in } k\text{-th coil ring,} \\ -i\omega \, \sigma_c \, \phi & \text{in other conductors,} \end{cases}$$

Global simulation – Temperature

axially symmetric and stationary temperature distribution

$$-\vec{\nabla}(\kappa\vec{\nabla}T) = f$$

with κ thermal conductivity, f heat sources (j^2/σ)

radiative heat transfer between surfaces of cavities:

$$\vec{q}_{\text{gas}}\,\vec{n} + R - J = \vec{q}_{\text{solid}}\,\vec{n}$$

R total outgoing radiation $R = \sigma\epsilon T^4 + (1-\epsilon)J$
J incoming radiation $J(x) = \int \Lambda(x,y)\,\omega(x,y)R(y)dy$

σ Boltzmann radiation constant, ϵ emissivity
$\Lambda(x,y) = 1$ if y is "visible" from x, 0 otherwise
$\omega(x,y)$ view factors

Global temperature distribution

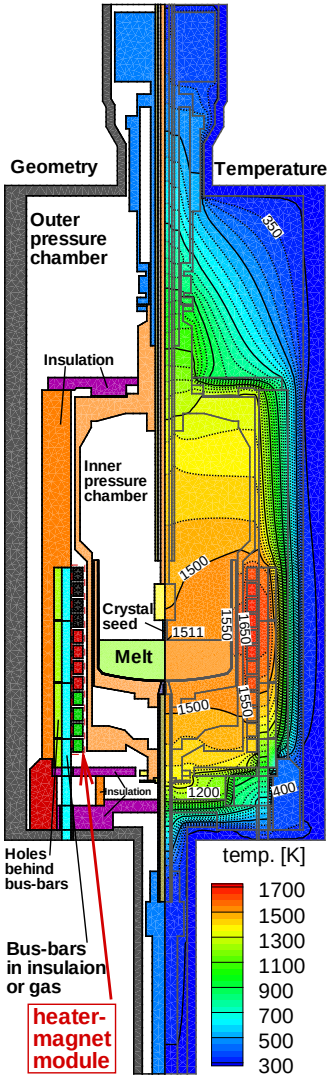

Asymmetry of heater magnet

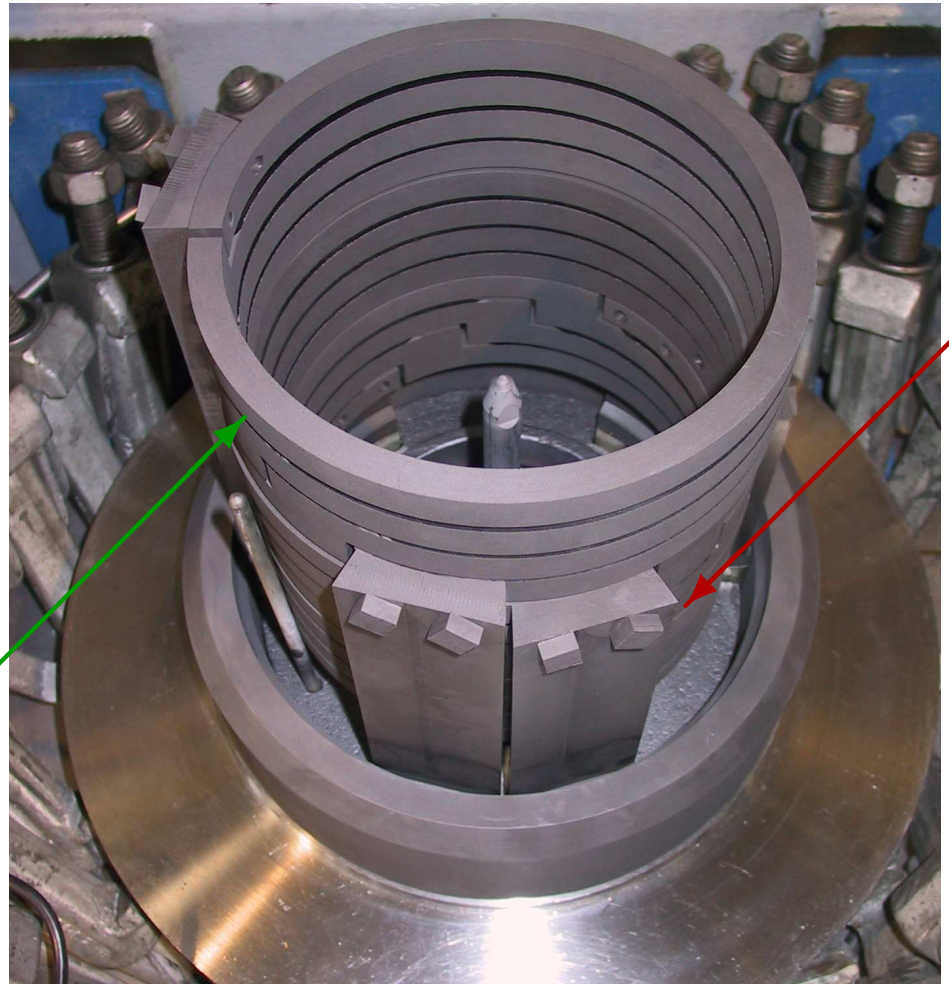

bus bars

not
axially symmetric

⇒ account for
asymmetries
in 2.5D simulations

heater
magnet

photo: IKZ

account for 3D effects

Model 1

ignore bus bars

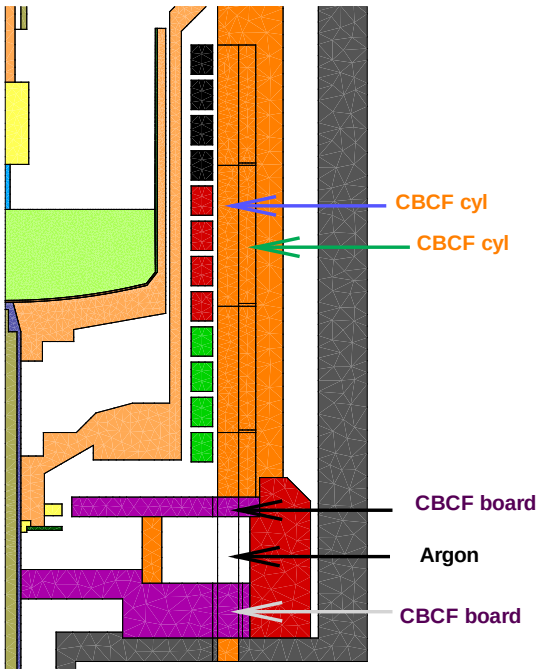

Model 2

bus bars: thin cylinder

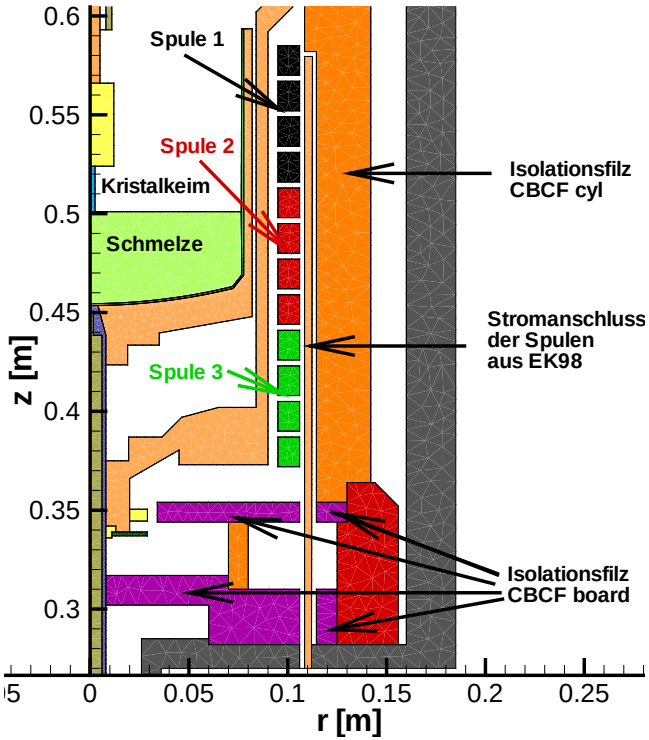

Model 3

average over materials

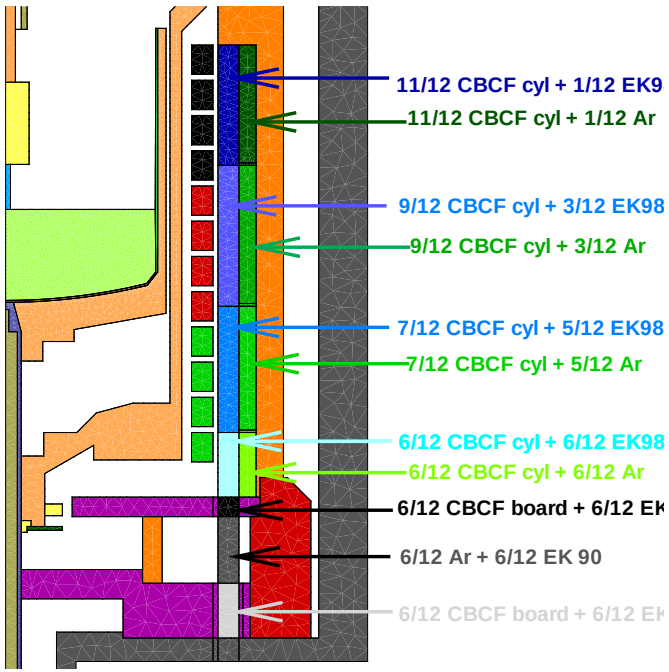

Local Simulation – Navier-Stokes equations, Boussinesq approximation

$$\partial_t \vec{u} + (\vec{u} \cdot \vec{\nabla})\vec{u} = -\vec{\nabla} p + \frac{1}{\mathrm{Re}} \Delta \vec{u} + \frac{\mathrm{Gr}}{\mathrm{Re}^2} T \vec{e}_z + \frac{L}{\rho_0 V^2} \vec{j} \times \vec{B}$$

$$\vec{\nabla} \vec{u} = 0$$

$$\partial_t T + (\vec{u} \cdot \vec{\nabla}) T = \frac{1}{\mathrm{Pr}\,\mathrm{Re}} \Delta T$$

with

- $\rho_0 = \rho(T_{melt})$, $p = (\tilde{p} + \rho_0 |\vec{g}| z)/(\rho_0 V^2)$, with $\tilde{p}$ pressure
- units $L, V, L/V$ for length, velocity, time, δT for temperature
- T difference to melting temperature
- $\mathrm{Re} := \frac{VL}{\nu}$ Reynolds number, $\mathrm{Gr} := \frac{\alpha \delta T g L^3}{\nu^2}$ Grashof number, $\mathrm{Pr} := \frac{\nu}{\chi}$ Prandtl number, $\mathrm{Pr} = 0.068$
- orders of magnitude: $\mathrm{Re} \sim 10^3 - 10^4$, $\mathrm{Gr} \sim 10^8$

Boundary Conditions

Temperature

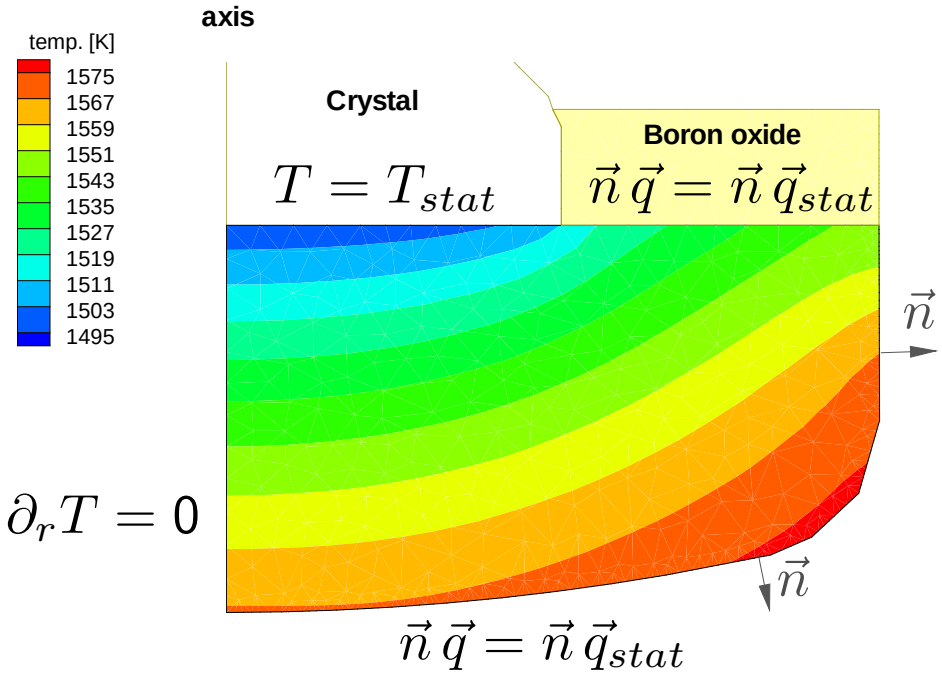

with encapsulant

radiation

$$\vec{n}\vec{q} = \vec{n}\vec{q}_{stat} + \sigma\epsilon(T^4 - T_{stat}^4)$$

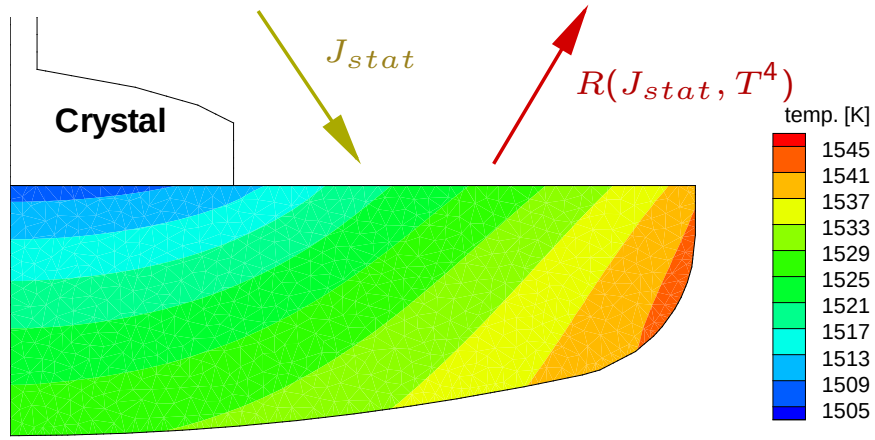

without encapsulant

$\vec{n}\vec{q} = -\kappa\,\vec{n}\vec{\nabla}T$, σ = Stefan-Boltzmann, ϵ = emissivity

Boundary Conditions

Velocity

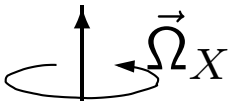

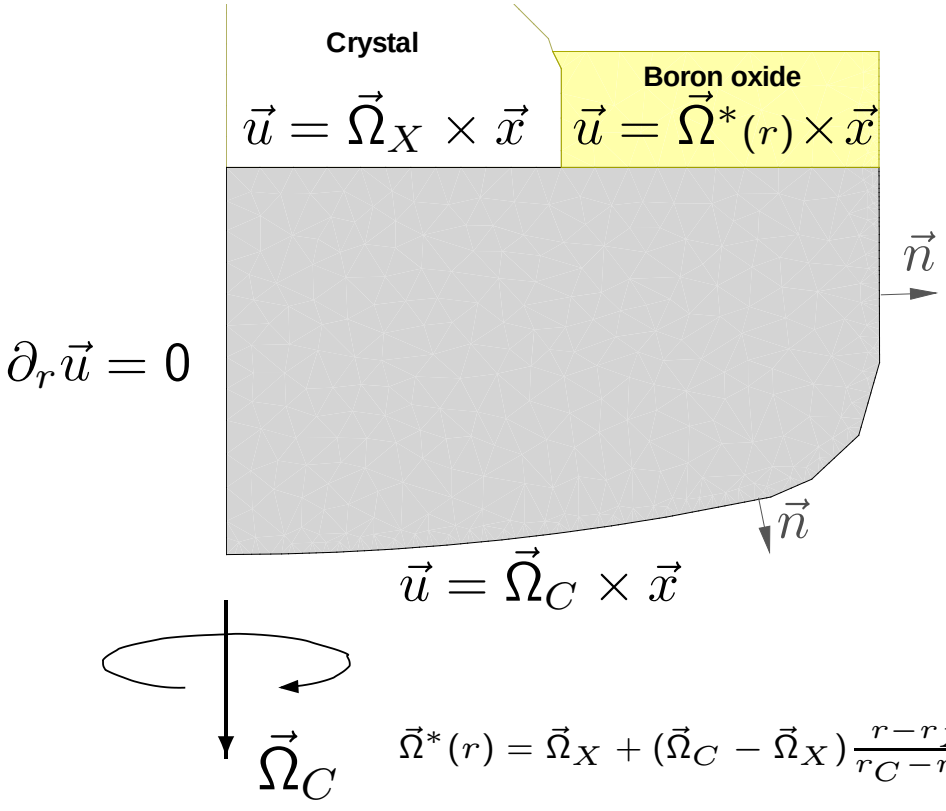

$$\vec{\Omega}^*(r) = \vec{\Omega}_X + (\vec{\Omega}_C - \vec{\Omega}_X)\frac{r - r_X}{r_C - r_X}$$

Marangoni convection

$$u^z = 0$$
$$\partial_z u^r = -\frac{\mathrm{Ma}}{\mathrm{Re\,Pr}} \partial_r T$$
$$\partial_z u^\varphi = 0$$

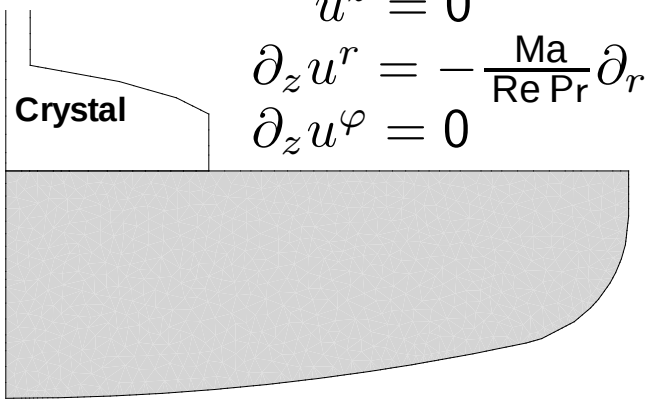

$$\mathrm{Ma} = (-\tfrac{\partial s}{\partial T})\tfrac{\delta T L}{\rho_0 \nu \chi}$$

without encapsulant

Plan

- Introduction
- Numerical Methods
- Comparison to experiments
  - Lorentz force
  - Temperature and input power
  - Melt surface
- Current investigations
- Summary

Lorentz force: experiment ↔ simulation

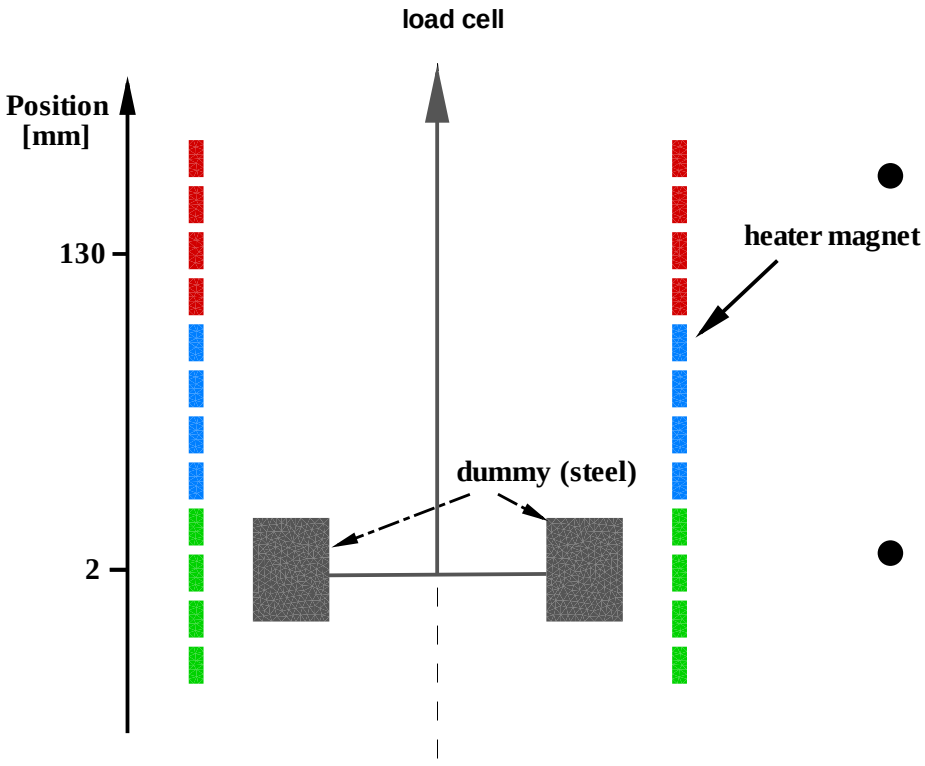

- expermiental data (2006):
  - dummy (steel) at various positions
  - TMF with various frequencies, phases

  load cell measures change in weight
- simulation:
  - IKZ: CrysVUn
  - WIAS: WIAS-HiTNIHS

Lorentz force: experiment ↔ simulation

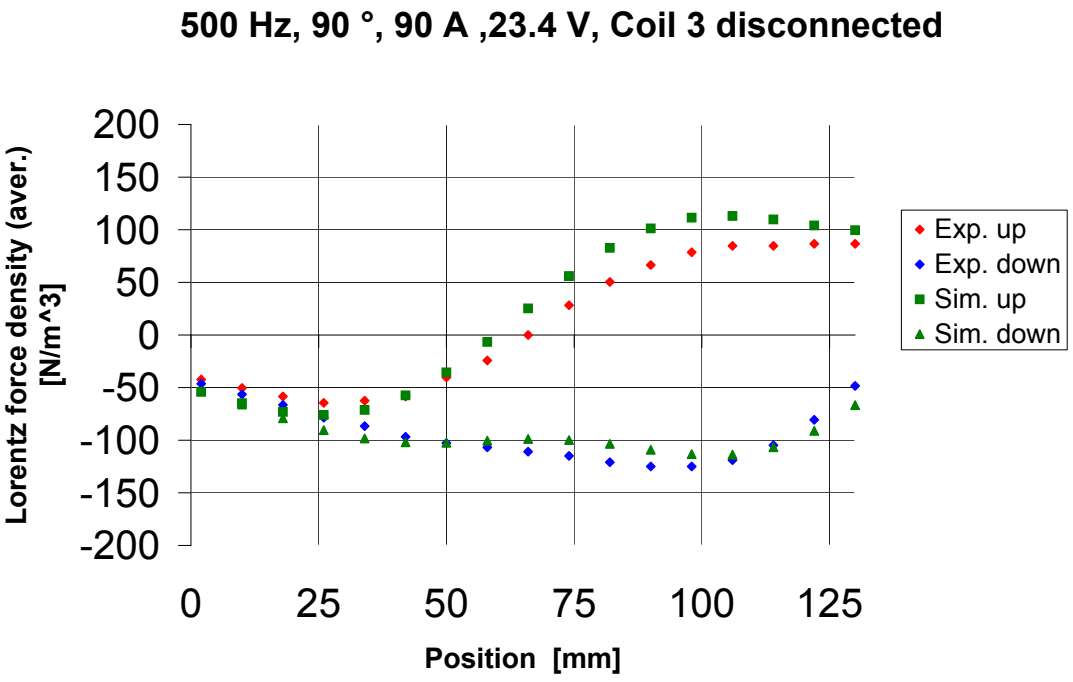

- $\vec{F}_L$ down: good agreement
- $\vec{F}_L$ up: simluation overestimates force systematically probably due to design of load cell
- gradients are reproduced well

Temperature distribution – compare models, experiment

model 1 (no bus bars)

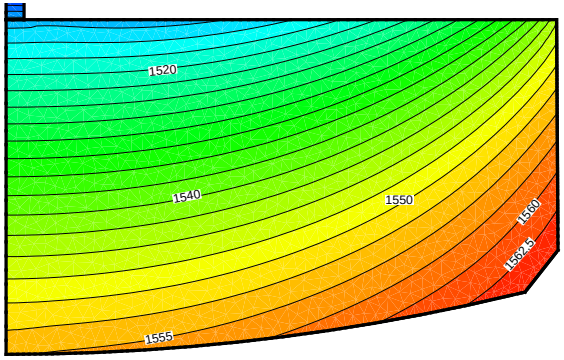

$P = 5.6\,\mathrm{kW}$

$\Delta T_{\mathrm{vert}} = 43\,\mathrm{K},$

$\Delta T_{\mathrm{horiz}} = 34\,\mathrm{K},$

$T_b = 1556\,\mathrm{K}, T_h = 1636\,\mathrm{K}$

model 2

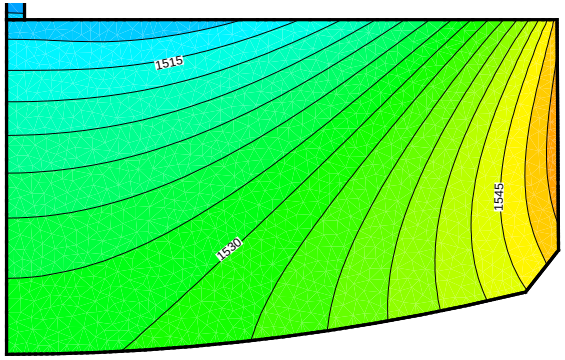

$P = 8\,\mathrm{kW}$

$\Delta T_{\mathrm{vert}} = 18\,\mathrm{K}$

$\Delta T_{\mathrm{horiz}} = 38\,\mathrm{K},$

$T_b = 1529\,\mathrm{K}, T_h = 1648\,\mathrm{K}$

model 3

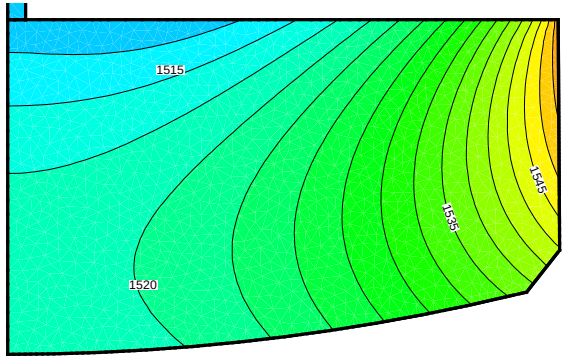

$P = 10\,\mathrm{kW}$

$\Delta T_{\mathrm{vert}} = 7\,\mathrm{K}$

$\Delta T_{\mathrm{horiz}} = 40\,\mathrm{K}$

$T_b = 1518\,\mathrm{K}, T_h = 1655\,\mathrm{K}$

- experimental data: $P = 9\,\mathrm{kW}, T_b = 1496\,\mathrm{K}, T_h = 1608\,\mathrm{K}$
- bus bars transport heat downwards
- models 2,3 give the rough picture, temperature distributions differ

Melt surface

Experiment: VCz without boron oxide, particles on free melt surface

- without TMF, particles cover the surface
- with TMF down: particles move outward
- with TMF up: particles come back in

Numerical simulation

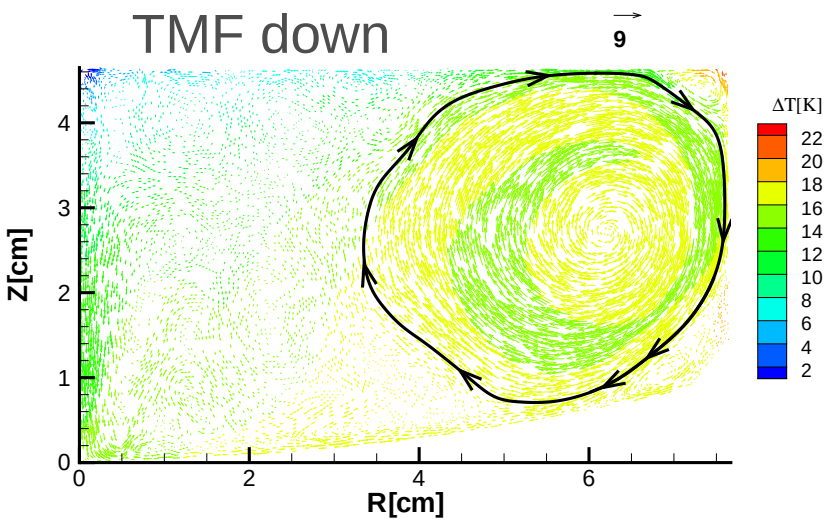

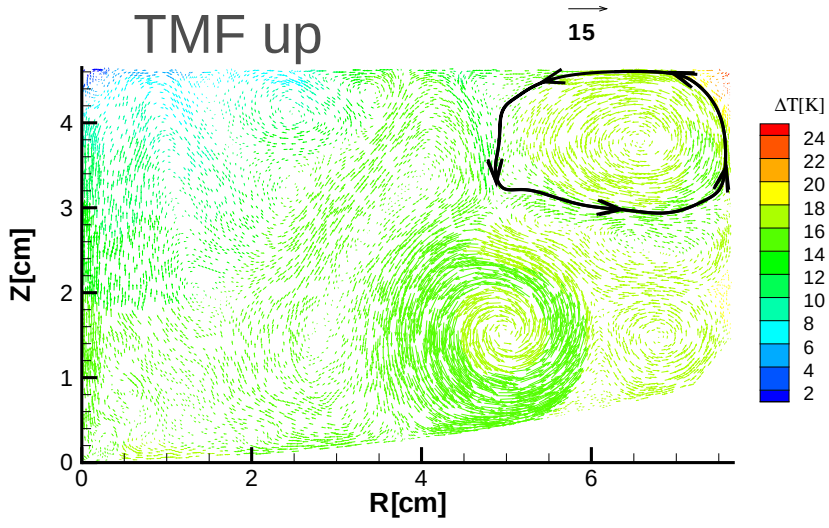

Plan

- Introduction
- Numerical Methods
- Comparison to experiments
- Current investigations
  - VCz growth of GaAs under the influence of TMFs
  - Numerical results
- Summary

VCz growth of GaAs under the influence of a TMF

VCz without B_2O_3, several crystals, e.g.

Spring 2007

TMF 400 Hz, 100° down

$\Omega_X = 5\,\text{rpm}, \Omega_C = -25\,\text{rpm}$

$v_{pull} = 5\,\text{mm/h}$

$\varnothing = 48 - 73\,\text{mm}$

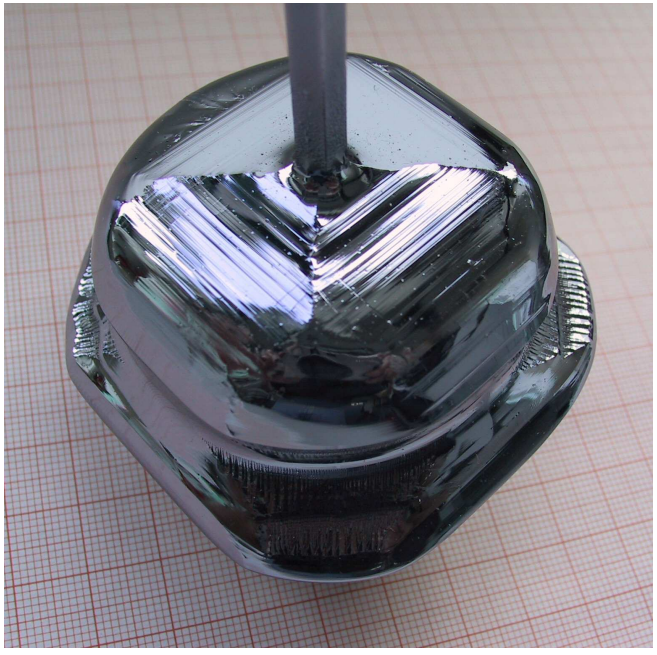

F. Kießling (IKZ)

VCz growth of GaAs, 400 Hz, 60° at $\Omega_C = -5$ rpm

crystal
(400 Hz, 60° down, −5 rpm)

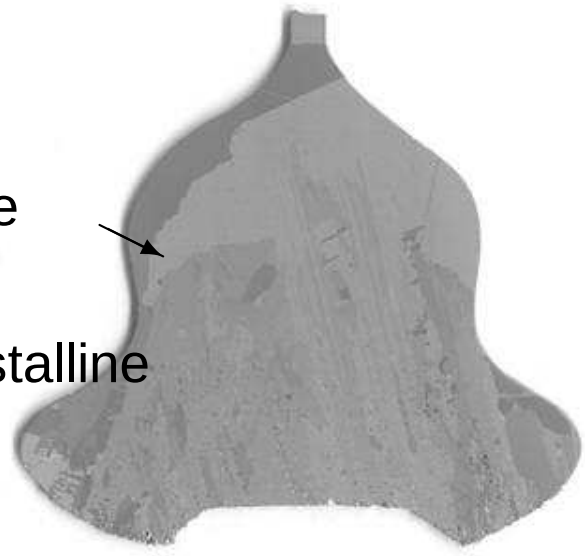

interface
concave

poly-crystalline

temperature oscillations

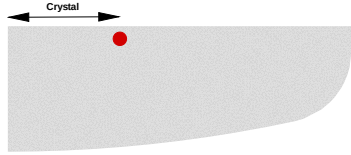

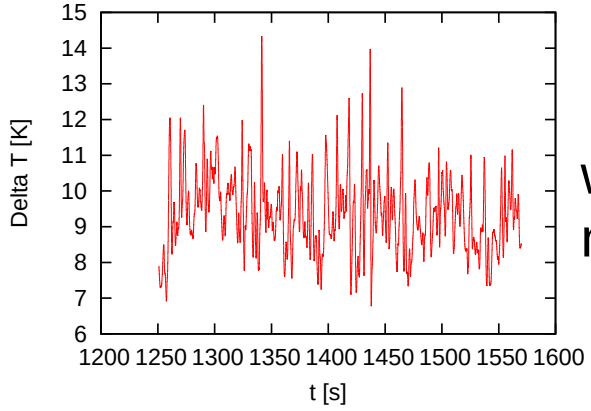

with TMF
magn. field too strong

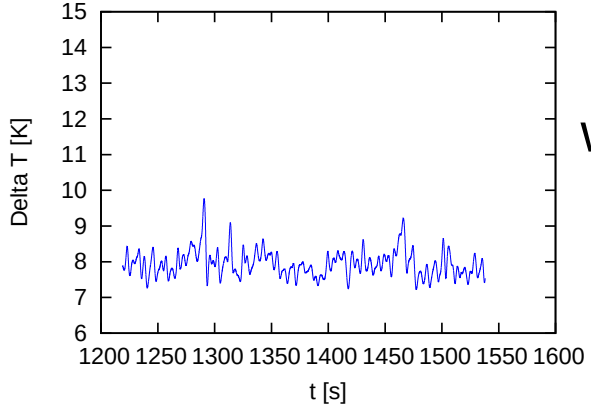

without Lorentz force

VCz growth of GaAs, $\Omega_C = -25$ rpm, TMF, various frequencies, phase shifts

400 Hz, 60°, down

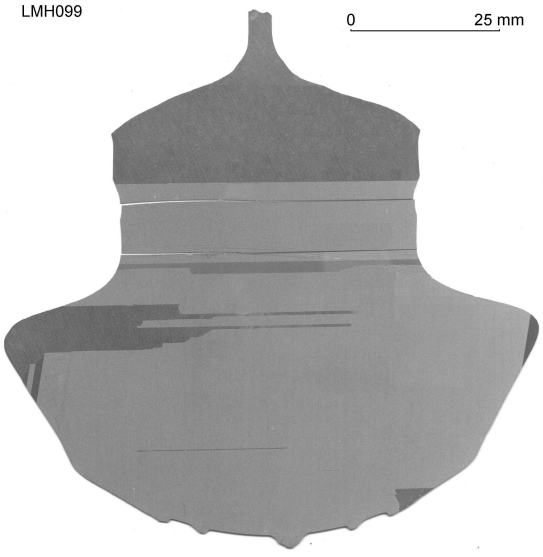

- interface almost planar
- striations homogenuous, small amplitude
  $\Rightarrow$ probably smaller fluctuations in the growth velocity v_g(T-oscill.)
  distance (in the upper part): $\sim 40\,\mu$m,
  $v_{pull} = 5$ mm/h
  $\Rightarrow$ T-oscillations with frequency ~ 0.035 Hz
  simulations for fixed melt height, various TMFs
- change in diameter
  $\Rightarrow$ due to change in flow pattern?
  simulations for various melt heights

Striation analysis, $\Omega_C = -25$ rpm

ohne WMF
-25 rpm

< 100 >

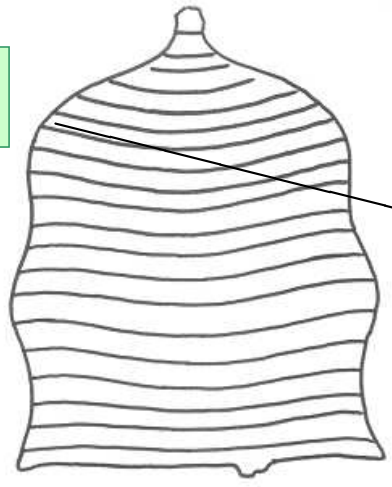

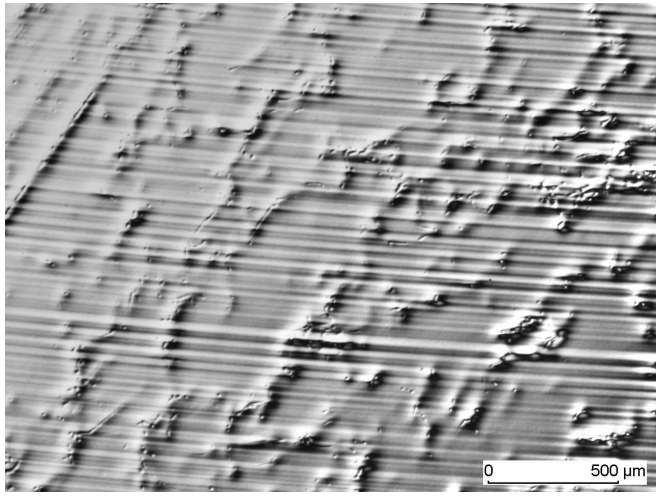

mit WMF
400 Hz, **110°**,
-25 rpm

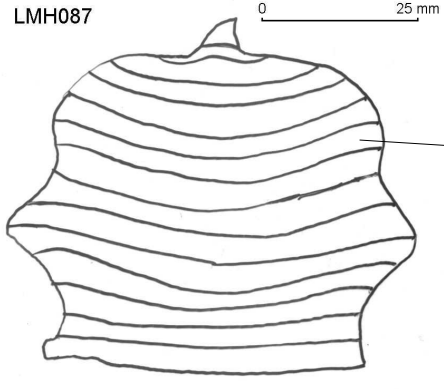

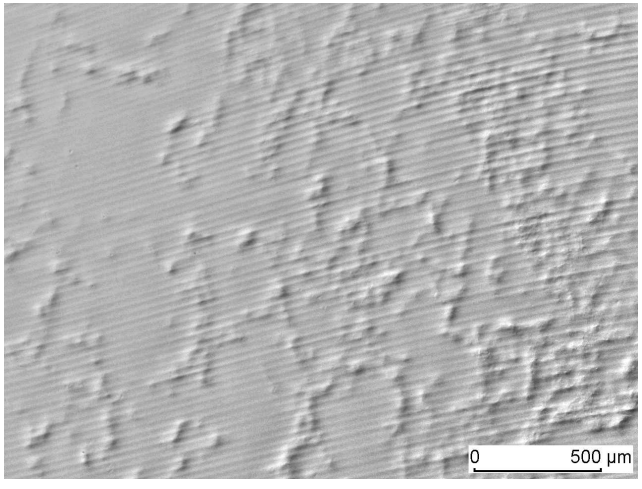

F. Kießling et.al
(IKZ)

Numerical simulation, TMF, 400 Hz, 110°, $\Omega_C = -25$ rpm

heat flux boundary conditions

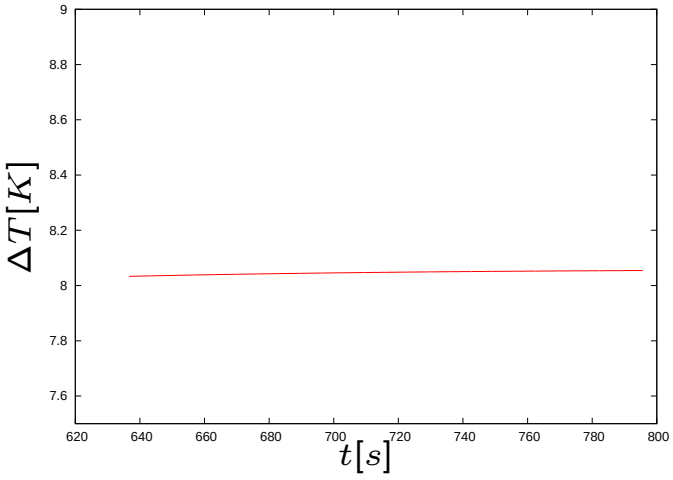

- stationary solution (dominated by Ω_C)
- not due to magnetic field

possible reasons

- axial symmetry $\rightarrow$ 3D
- $(\Delta T)_{axial}$ too small
  - simulation: $(\Delta T)_{axial} \sim 8$ K
  - experiment: $(\Delta T)_{axial} \sim 30$ K

Dirichlet boundary conditions

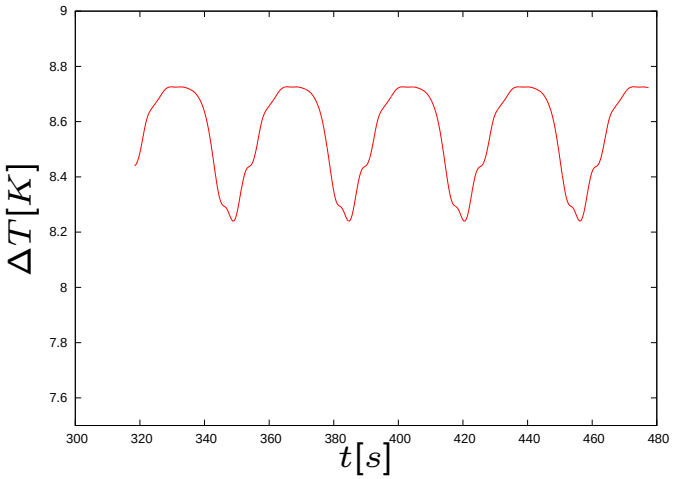

- $(\Delta T)_{axial} = 20$ K
- still dominated by Ω_C
- small fluctuations in the temperature
- frequency $f \sim 0.0277$ Hz $\rightarrow \sim 50\,\mu$m

3D simulation

- $\Omega_X = 6\,\text{rpm}, \Omega_C = -25\,\text{rpm}$
- no magnetic field
- heat flux boundary conditions
- no marangoni convection
- slight deviation from axial symmetry in the inner part
- axially symmetric in the outer part

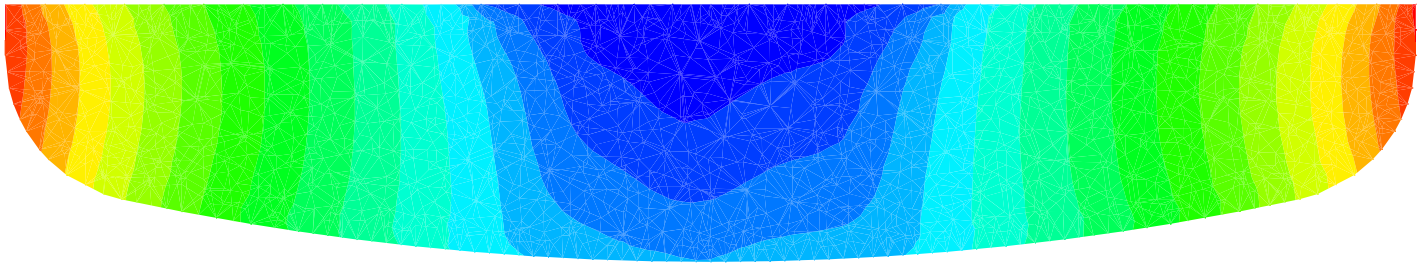

Numerical simulation of Czochralski crystal growth

- global stationary simulation for electro-magnetic quantities, temperature distribution
- local transient simulation
- good reproduction of electro-magnetic quantities (Lorentz force)
- global simulation of the temperature distribution (at the moment) gives a rough picture
- local axially symmetric simulation of the melt flow and temperature distribution
  - agrees with some of the experimental results
  - is not convincing (as compared to experiments) for small heights of the melt and high rotation rates